Journal of Medicinal Chemistry

Volume 49, Number 6 March 23, 2006

Articles

A Multistep Approach to Structure-Based Drug Design: Studying Ligand Binding at the Human Neutrophil Elastase†

Thomas Steinbrecher,‡ David A. Case,§ and Andreas Labahn*,‡

Institut für Physikalische Chemie, Albert-Ludwigs-Universität Freiburg, Albertstrasse 23a, 79104 Freiburg, Germany, and Department of Molecular Biology, The Scripps Research Institute, 10550 North Torrey Pines Road, La Jolla, California 92037

Received June 17, 2005

In this study we show that a combination of different theoretical methods is a viable approach to calculate the binding affinities of new ligands for the human neutrophile elastase. This protease degrades elastin and likely aids neutrophils in fulfilling their immunological functions. Abnormally high human neutrophil elastase (HNE) levels are involved in several diseases; therefore, inhibitors of HNE are of interest as targets for drug design. A recent study has revealed that cinnamic acid and bornyl ester derivatives bind to HNE, but ΔG^0 values from ligand docking results exhibited no correlation with those calculated from the IC_{50} values. To accurately compute binding affinities, we generated possible protein ligand complex structures by ligand docking calculations. For each of the ligands, the 30 most likely placements were used as starting points of nanosecond length molecular dynamics simulations. The binding free energies for these complex structures were estimated using a continuum solvent (MM-PBSA) approach. These results, along with structural data from the molecular dynamics runs, allowed the identification of a group of similar placements that serve as a model for the natural protein ligand complex structure. This structural model was used to perform thermodynamic integration (TI) calculations to obtain the relative binding free energies of similar ligands to HNE. The TI results were in quantitative agreement with the measured binding affinities. Thus, the presented approach can be used to generate a probable complex structure for known ligands to HNE and to use such a structure to calculate the effects of small ligand modifications on ligand binding, possibly leading to new inhibitors with improved binding affinities.

Introduction

The human neutrophil elastase is a serine protease that is produced in the most abundant of white blood cells, the granulocytes. Its function in the immune system lies in the defense against pathogenes and foreign protein material.[1,2] HNE's specificity for cleavage after small aliphatic amino acid residues, especially valine, enables it to hydrolyze a wide variety of protein substrates, notably elastin, a protein that gives skin its elastic properties.

HNE is a soluble, small protein of ca. 30 kDa size. The functional enzyme contains 218 amino acid residues, organized into two domains of beta-barrels, and is stabilized by four disulfide bridges. About 20% of the protein mass is made up of two carbohydrate chains of variable sequence.[3,4] Nineteen arginine residues on the protein surface and only nine acidic residues make it a highly basic protein. Several X-ray crystal structures of HNE complexed with different inhibitors have been solved to atomic resolution.[5−7]

The activity of HNE released from granulocytes is tightly regulated by several inhibitors,[8] but in tissues massively infiltrated by neutrophils this regulation can be insufficient. High

† Dedicated on the occasion of the 80th birthday of Prof. Dr. Dr. h.c. Gerhart Drews.

* To whom correspondence should be addressed. Phone: +49 761 203 6188. Fax: +49 761 203 6189. E-mail: andreas.labahn@physchem.uni-freiburg.de.

‡ Albert-Ludwigs-Universität Freiburg.

§ The Scripps Research Institute.

10.1021/jm0505720 CCC: $33.50
Published on Web 02/16/2006

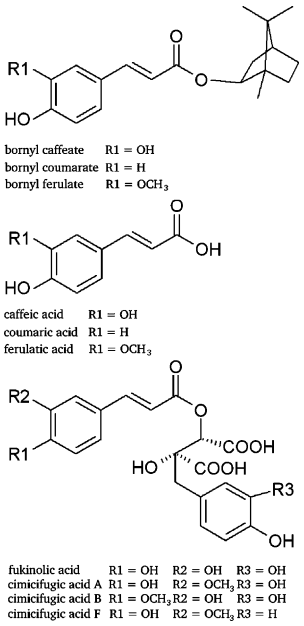

Figure 1. Several known inhibitors to HNE. Three groups of ligands, differing only in their substitution patterns, can be distinguished: bornyl esters of caffeic acid derivatives (top), caffeic acid derivatives (middle), and fukinolic acid derivatives (bottom).

levels of unregulated HNE can cause degradation of healthy tissues and result in the development of diseases such as pulmonary emphysema, cystic fibrosis, or rheumatoid arthritis.[9,10] Thus, new inhibitors of HNE are of considerable interest for the development of anti-inflammatory drugs.

Recently, cinnamic acid ester derivatives as well as cimicifugic acid derivatives have been shown to inhibit HNE with IC_{50} values in the μM range.[11,12] Structure activity relationship studies gave some insight into the molecular mechanism underlying the pharmacological effects, but a quantitative description of experimental differences in binding free energies for the different ligands could not be found.[13]

In this study we have used a combination of ligand docking calculations and molecular mechanics simulations to evaluate likely complex structures for HNE and several of its inhibitors. The relative binding affinities for different ligands were accurately calculated by thermodynamic integration calculations. This method has been employed successfully in biophysical studies to predict free energy changes,[14,15] notably the effect of amino acid point mutations.[16] Here, we report one of the few cases of thermodynamic integration calculations as a tool to derive quantitative values of differences in binding free energies for ligands. While our approach is computationally demanding and thus not useful for virtual screening experiments, it can be applied for virtual ligand optimization, after a lead compound has been identified.

Results

Ligand Docking and MD Calculations. Ligand docking calculations were performed with several known inhibitors of HNE (Figure 1). For the 10 ligands, the 30 best placements in each case were analyzed. For each ligand, a wide variety of binding conformations were found, most of them not situated close to the active center of the protein binding pocket, with observed distances in the range of 4−12 Å. For several ligands, e.g., bornyl ferulate, which is known to inhibit HNE, no reasonable placement of the ligand in the binding pocket was observed at all. For the three very similar bornyl ester type ligands, widely differing placements were found and only for bornyl caffeate binding of the ligand within the active site was predicted. The estimates of the binding free energies from the docking scoring function were in the range of −3 to −5 kcal/mol and were not in qualitative agreement with the experimental values of the binding free energies derived from known IC_{50} values, as reported earlier.[13]

Starting from several of the best placements for each ligand, 2 ns length MD simulations were performed and structural snapshots were taken and evaluated by the MM-PBSA method. In these simulations many of the ligand placements proved unstable during unrestrained simulation conditions with the ligand moving around more than 5 Å on the protein surface or even completely dissociating from the protein.

The ΔG^0_{Bind} values calculated from these simulations did not agree with experimental data (comparison not shown). Therefore, a more thorough analysis was necessary. For the two compounds with the lowest IC_{50} values, bornyl caffeate and fukinolic acid, the 30 best docking placements were clustered into placement groups in a way that each placement in a group had an rmsd of <4 Å to all other group placements (Figure 2). For both ligands, the number of placements in each group varied widely, ranging from up to 16 conformations down to a single one.

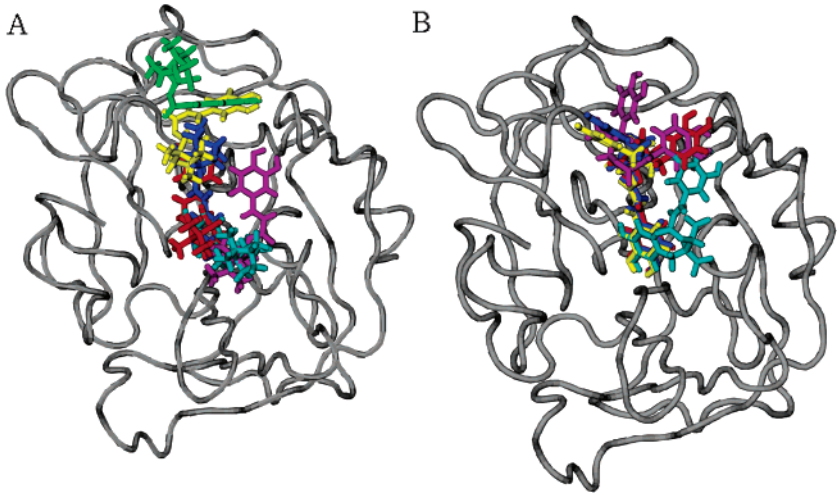

Figure 2. Ligand placement groups for bornyl caffeate (A) and fukinolic acid (B) obtained by combining similar docking placements. The protein backbone is depicted as a gray tube and the different ligand placements in color. For bornyl caffeate six placement groups were found and for fukinolic acid five.

Table 1. MD Simulations and MM-PBSA Derived $\Delta G^{0\prime}$ Values for the Different Ligand Placement Groups of Bornyl Caffeate[a]

group	simulations total	simulations stable	$\Delta G^{0\prime}_{Avg}$ [kcal/mol]	$\sigma(\Delta G^{0\prime})$ [kcal/mol]
1	16	10	−15.5	3.5
2	7	7	−19.8	0.8
3	2	1	−16.5	
4	1	0		
5	3	3	−8.6	1.0
6	1	0		

[a] Group refers to the ligand placement groups generated by combining similar docking solutions. Simulations give the number of ligand placements in a group and the number of simulations that showed a stable ligand placement over 1 ns. $\Delta G^{0\prime}_{Avg}$ and $\sigma(\Delta G^{0\prime})$ are the average free energies of all stable simulations and their standard deviation, respectively.

Molecular Dynamics Simulation with Bornyl Caffeate. For bornyl caffeate a 1 ns length MD simulation was performed for each of the ligand placements in each group. During all simulations, the rmsd of the protein compared to its initial structure was below 2 Å (see Supporting Information for examples of a protein ligand complex structure before and after MD simulation). B-values calculated from the atomic fluctuations were in the 10−30 Å^2 range, with few mobile surface residues reaching 60−80 Å^2.

The rmsd values of the ligands in all simulations, compared to their starting points, were monitored and only those simulations in which the ligand exhibited a stable binding position were considered for further analysis. A stable binding position was defined by the ligand still being within 4 Å rmsd of all other stable ligand placements in its group at the end of the 1 ns MD simulation. The different placement groups displayed markedly different numbers of stable to total simulations. For each stable simulation the binding free energy was calculated from structural snapshots by the MM-PBSA method (Table 1). The second group of ligand placements exhibited a significantly more negative average binding free energy than all other simulations. The resulting binding free energies for the individual placements in group 2 were very similar, with a mean deviation of less than 5%. Furthermore, in placement group 2 only stable simulations (100%) were observed, while in group 1 only 63% of the simulations were stable. Therefore, we regarded the ensemble of ligand placements that formed placement group 2 as the most reasonable model for the binding geometry of bornyl caffeate and used it as starting geometry for all further simulations.

In our proposed binding mode (Figure 3) the caffeic acid part of bornyl caffeate occupies the catalytic center, with the two hydroxyl groups placed close to the oxyanion hole made up by Gly 193 and Ser 195. The bornyl residue is placed close to lipophilic residues of the enzyme S1 specificity pocket. An analysis of protein ligand hydrogen bonds formed during the MD simulations was performed. For each of the seven group 2 simulations, 100 structural snapshots were considered. Three hydrogen bonds were found to be present in more than 600 snapshots: A hydrogen bond from the backbone NH-group of Val 216 to the carbonyl oxygen atom of the bornyl caffeate ester group (found in 700 snapshots) and two hydrogen bonds involving the meta-OH group of bornyl caffeate, one as a hydrogen donor to the backbone carbonyl O-atom of Phe 41 (646 snapshots) and one as a hydrogen acceptor from the backbone NH-group of Gly 193 (634 snapshots). Three weaker hydrogen bonds were found to be present in less than 100 of the structural snapshots; these were formed between the backbone carbonyl O-atom of Phe 41 and the para-OH group of bornyl caffeate (71 snapshots), between the NH-group of Ser 195 and the meta-O-atom of bornyl caffeate (41 snapshots) and between the γ-O-atom of Ser 195 and the meta-OH group of bornyl caffeate (25 snapshots).

A 1 ns MD simulation for both bornyl ferulate and bornyl coumarate was conducted using the respective ligand modeled onto the binding geometry of the group 2 placement of bornyl caffeate as starting point because no placements similar to the best binding geometry of bornyl caffeate were found in the ligand docking results for the other two borneol ester type ligands. Both simulations showed a stable binding configuration for the whole simulation time with both ligand rmsd's compared to the starting structure at ∼2 Å. MM-PBSA binding free energies were calculated according to eq 1. The results of −19.8 and −20.4 kcal/mol for bornyl coumarate and bornyl ferulate respectively are very close to the $\Delta G^{0\prime}$ result for bornyl caffeate −19.8 ± 0.8 kcal/mol. We thus concluded that the group 2 placement geometry of bornyl caffeate is a viable binding model for the three similar ligands bornyl caffeate, bornyl coumarate, and bornyl ferulate.

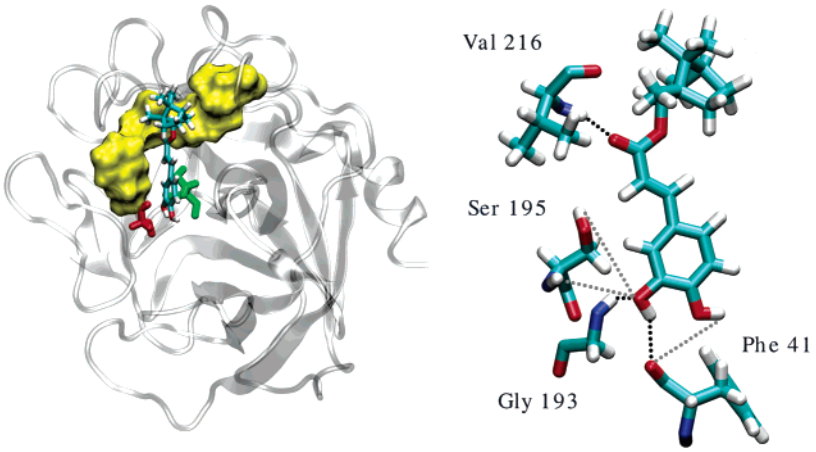

Figure 3. The binding mode of bornyl caffeate as derived from MM-PBSA calculations. Left: The bornyl moiety of the ligand is placed close to lipophilic amino acids of the enzyme specificity pocket (amino acid residues Leu 99, Phe 192, Phe 215, and Val 216 are depicted in yellow surface representation), the two hydroxyl groups of the caffeic acid part are located close to the oxyanion hole in the binding pocket (formed by the NH groups of amino acid residues Gly 193 and Ser 195 which are depicted in red and green, respectively). Right: Three important hydrogen bonds (black) are observed during MD simulations; the backbone functional groups of Phe 41, Gly 193, and Val 216 anchor the ligand to the binding site. Three less important hydrogen bonds (gray) involving Phe 41 and Ser 195 are only observed in some of the MD snapshots.

Table 2. Free Energy Changes from Thermodynamic Integration Calculations for the Transformation of Bornyl Caffeate to Bornyl Coumarate and Bornyl Ferulate to Bornyl Caffeate Compared to Experimental Values Calculated from Differences in IC_{50} Values[a]

transformation	ΔG^0_{Step1} [kcal/mol]	ΔG^0_{Step2} [kcal/mol]	ΔG^0_{Total} [kcal/mol]	$\Delta\Delta G^0_{Bind}$ [kcal/mol]	$\Delta\Delta G^0_{Exp}$ [kcal/mol]
Bornyl Caffeate−Bornyl Coumarate					
free solvated ligand	−20.5	−0.9	−21.4		
4 different ligand placements for bound bornyl caffeate	−18.0	−0.8	−18.8		
	−17.6	−1.4	−19.0	+2.0 ± 0.5	+2.3
	−19.1	−0.9	−20.0		
	−18.4	−1.2	−19.6		
complexed ligand average	−18.3	−1.1	−19.4		
Bornyl Ferulate−Bornyl Caffeate					
free solvated ligand	−6.1	−3.8	−9.9		
4 different ligand placements for bound bornyl ferulate	−6.4	−6.9	−13.3		
	−6.2	−8.8	−15.0	−3.3 ± 1.2	−2.4
	−6.3	−6.0	−12.3		
	−6.4	−5.6	−12.0		
complexed ligand average	−6.3	−6.8	−13.2		

[a] For a given IC_{50} value taken from refs 11 and 12, the corresponding free energy was obtained from $\Delta G^0 = RT \ln(IC_{50})$.

TI Calculations with Bornyl Caffeate Derivatives. The relative binding free energies for the three bornyl caffeate derivatives were determined by TI calculations (Table 2). For the protein-bound ligands, four simulations were started both for the transformation of bornyl caffeate to bornyl coumarate and bornyl ferulate to bornyl caffeate, while for the free solvated ligands only one simulation per ligand transformation was performed. For each simulation of a complexed ligand a different starting geometry was selected from the seven group 2 placements of bornyl caffeate. In the case of the bornyl ferulate to bornyl caffeate simulation the starting geometry of bornyl ferulate was modeled onto the bornyl caffeate placement.

For both ligand transformations the free energy changes calculated in the four protein ligand complex simulations were averaged and the relative binding free energy was calculated according to eq 4. The standard deviation, calculated for the ΔG^0 values of the protein bound ligand transformations, is 0.5 kcal/mol for bornyl caffeate/bornyl coumarate and 1.2 kcal/mol for bornyl ferulate/bornyl caffeate. When the results are compared to experimentally determined differences in binding free energy, calculated from the IC_{50} values taken from,[11,12] the result for the bornyl caffeate to bornyl coumarate transformation of +2.0 kcal/mol is in good agreement with the experimental difference of +2.3 kcal/mol, taking the standard deviation into account. For the bornyl ferulate to bornyl caffeate transformation, the experimental value of −2.4 kcal/mol is in reasonable agreement with the calculated free energy difference of −3.3 ± 1.2 kcal/mol. Furthermore, a geometric reason can be found for the overly preferential binding of bornyl caffeate. In Figure 3, the meta-hydroxy group of bornyl caffeate is depicted close to the protein surface and interacting with binding pocket amino acid residues. While this placement is sensible for bornyl caffeate, for the placement of bornyl ferulate (which was generated from the top placement of bornyl caffeate) another position for the meta-substituent (then a methoxy instead of a hydroxy group) can be considered, consisting of flipping the aromatic residue by 180° along its longitudinal axis (vertical in Figure 3) without changing the position of the remainder of the ligand. To calculate the free energy difference of these two placements for bornyl ferulate, the free energy profile for rotating the aromatic moiety could be calculated by means of umbrella sampling[17] or similar techniques. Alternatively, the free energy difference can be estimated by a sequence of TI calculations (Figure 4): For bornyl ferulate in the alternative (flipped) position, a ligand transformation to bornyl caffeate was simulated (Step D). For the flipped bornyl caffeate, the transformation to bornyl coumarate was also simulated (Step C). Due to the C_2 symmetry of the aromatic moiety in bornyl coumarate, the difference of the free energy change for the two transformations of flipped ligands and the two transformations of the regularly placed ligands should equal the free energy change of flipping the bornyl ferulate aromatic residue. The TI calculations resulted in ΔG^0 values of −9.8 kcal/mol for the transformation of flipped bornyl ferulate to flipped bornyl caffeate (Step D) and −21.2 kcal/mol for flipped bornyl caffeate to bornyl coumarate (Step C). Using the ΔG^0 values of −13.2 and −19.4 kcal/mol for the respective transformations (Step A and B) of the regularly placed ligands (see Table 2), a total ΔG^0 value of −1.6 kcal/mol for flipping the bornyl ferulate aromatic residue so that the methoxy group faces the surrounding solvent instead of the binding site surface is obtained. If

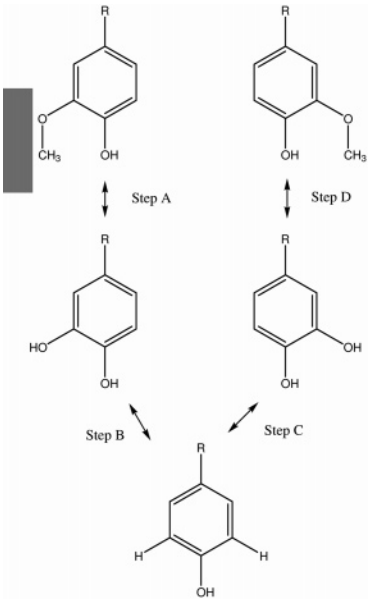

Figure 4. The sequence of TI calculations used to estimate the free energy change for turning the aromatic moiety of bornyl ferulate by 180° around its longitudinal axis. The top two steps A and D correspond to transformations of bornyl ferulate to bornyl caffeate beginning from two different starting positions, while the lower two steps B and C correspond to transformations of bornyl caffeate to bornyl coumarate. The gray bar indicates the sterical hindrance where the methoxy group of bornyl ferulate clashes with the binding site.

Table 3. MD Simulations and MM-PBSA Derived $\Delta G^{0\prime}$ Values for the Different Ligand Placement Groups of Fukinolic Acid[a]

group	simulations total	simulations stable	$\Delta G^{0\prime}_{Avg}$ [kcal/mol]	$\sigma(\Delta G^{0\prime})$ [kcal/mol]
1	10	6	−8.1	4.8
2	12	3	−11.9	2.1
5	4	3	−14.8	5.2

[a] Group refers to the ligand placement groups generated by combining similar docking solutions. Simulations give the number of ligand placements in a group and the number of simulations that showed a stable ligand placement over 1 ns. $\Delta G^{0\prime}_{Avg}$ and $\sigma(\Delta G^{0\prime})$ are the average free energies of all stable simulations and their standard deviation, respectively.

one takes this alternative binding mode of bornyl ferulate into account, the $\Delta\Delta G^0$ for the binding of bornyl ferulate and bornyl caffeate changes from +3.3 to +1.7 kcal/mol, now slightly less than the experimental value of +2.4 kcal/mol, but still within the standard deviation estimated above. This shows that the deviation of calculated and experimental results in this case can be attributed to small conformational changes in the ligand binding modes. It is notable that such conformational changes can be identified and their effects calculated by computational means only.

To test the effect the bornyl residue has on the binding free energies, a ligand transformation from bornyl caffeate to free caffeic acid was simulated, both in the solvated state and with different bornyl caffeate group 2 placements for the protein-bound state. The calculated $\Delta\Delta G^0$ was greater than +10 kcal/mol, significantly more than the expected amount from experimental data of +2.5 kcal/mol. An analysis of the free energy contributions shows that most of the $\Delta\Delta G^0$ is caused by the electrostatic changes during the transformation, likely due to the emerging negative charge on the caffeic acid at a position in the binding site where the much less polar ester group of bornyl caffeate was situated before. Such a lack of stabilization for caffeic acid in this binding mode indicates that our proposed binding mode for bornyl caffeate derivatives is not a valid model for the corresponding free acids.

Simulations with Fucinolic Acid Derivatives. A reasonable binding mode for fukinolic acid and its derivatives cimicifugic acid A, B, and F was searched for by an MM-PBSA reranking of the different groups of ligand placements from docking calculations with the ligand with the highest binding affinity to HNE, fukinolic acid, similar to the process for the bornyl caffeate derivatives. The three placement groups considered for fukinolic acid were not completely different; all placements had the aromatic residue of the caffeic acid part placed into the binding site at a position similar to that of the corresponding part of bornyl caffeate in the group 2 placements described above. Four of the top 30 docking placements of fukinolic acid, forming placement groups 3 and 4, that exhibited improbable placements far from the binding site were omitted from the calculations. The $\Delta G^{0\prime}$ values derived from 1 ns MD simulations of the different ligand placements according to eq 1 do not show a clear distinction between the groups (Table 3). Compared to the results from Table 1, lower $\Delta G^{0\prime}$ values, a lower percentage of stable simulations and higher variation of the calculated binding energies within the different groups make it difficult to distinguish one placement group as the most reasonable binding model for fukinolic acid.

Therefore, TI calculations were performed for the one placement of each group that exhibited the most negative $\Delta G^{0\prime}$ value, as well as for all placements of group 5 with the highest average $\Delta G^{0\prime}$. A total of three different ligand transformations were studied (Table 4). The results showed no good correlation

Table 4. Free Energy Changes Derived from TI Calculations for the Ligand Transformations of Different Fukinolic Acid Derivatives Compared to Experimental Values Calculated from Differences in IC_{50} Values Taken from refs 11 and 12[a]

ligand transformation	$\Delta\Delta G^0$ [kcal/ mol] group 1	group 2	group 5	$\Delta\Delta G^0_{Exp}$ [kcal/mol]
cimicifugic acid A−fukinolic acid	+2.5	+0.0	−1.6	−1.3
cimicifugic acid B−fukinolic acid	−0.2	−2.3	−0.1	−2.3
cimicifugic acid A−cimicifugic acid F	−0.4	+0.1	−0.1	+1.3

[a] $\Delta\Delta G^0$ is the free energy difference between the ΔG^0 of the transformation of ligand bound to the protein in one of three different binding modes and the ΔG^0 for the transformation of the solvated ligand. $\Delta\Delta G^0_{Exp}$ is the difference in binding free energy determined from experimental values.

of theoretical and experimental binding free energies for either one of the binding modes, preventing us from selecting one of them as a good model for the binding geometry of fukinolic acid.

Discussion

From ligand docking calculations alone no valid complex structures for HNE and its inhibitors could be derived and the binding scores from the docking process did not show qualitative correlation to binding affinities known from experimental data, as described before.[13] The reranking of the clustered ligand docking results with MM-PBSA free energy calculations resulted in the discovery of one binding mode for bornyl caffeate that exhibited markedly stronger binding free energies and significantly more stable complex MD simulations. Our final proposed binding mode did not include the docking solution that exhibited the most negative binding score but was combined from 7 of the 30 best docking solutions.

The MM-PBSA reranking of results did take protein flexibility into account. This is a significant contribution to improved scoring.[18] Another reason for improved results after the MM-PBSA step can be that the force field used in combination with continuum solvent electrostatics to calculate $\Delta G^{0\prime}$ provides a more accurate description of the ligand binding process than the empirical scoring function of the docking program.

It is notable however that the MM-PBSA results obtained from MD simulations with very similar starting structures fluctuated by 3.5 kcal/mol for one of the studied ligand placement groups and by almost 1 kcal/mol for the found binding model of bornyl caffeate. These fluctuations were small enough to distinguish between suitable and nonsuitable binding modes of bornyl caffeate; however, for fukinolic acid the fluctuations were too large to definitely select one of the tested binding modes as the most reasonable.

Since the MM-PBSA results fluctuated by 1 kcal/mol for different simulations of similar placements of the same ligand binding to HNE, MM-PBSA is not well-suited for the comparison of different ligands in similar binding modes since errors there will most likely be larger than 1 kcal/mol with experimental differences in the range of only 1−2 kcal/mol. Since MM-PBSA was employed for the accurate calculation of binding free energies before,[19] this result was unexpected. From the simulations performed here, it could not be concluded if this finding was caused by the biochemical system and simulation protocol used or if it represents some common attribute of the MM-PBSA method.

The bornyl residue of bornyl caffeate was found to be important for ligand binding; our results indicate that the free caffeic acid does not bind with a conformation similar to that of the esterified acids. The placement of the hydrophobic bornyl

residue into the S1 specificity pocket gives a structural explanation for the importance of ligand hydrophobicity for good binding to HNE, which was predicted by QSAR studies.[20]

Two similar possible binding modes were proposed for bornyl ferulate; the one more similar to the binding mode of bornyl caffeate seems to be less favorable than the one with a flipped aromatic residue. Further studies might calculate a more accurate relative free energy for both binding conformations either by averaging over more TI calculations or by obtaining the free energy profile for the aromatic residue flipping by means of umbrella sampling calculations.[17]

For fukinolic acid and its derivatives no unambiguous ligand placement could be distinguished by MM-PBSA reranking of the three studied placement groups and also none of the TI calculations with different binding conformations could reproduce experimental differences in binding free energies. The fact that the ligand placements from the docking calculations were very similar for fukinolic acid highlights the need for a diverse set of starting conformations before MM-PBSA reranking takes place. We suggest that not only the total free energy $\Delta G^{0\prime}$ from MM-PBSA calculations should be taken into account when selecting a model for the binding geometry but also the complex stability during the corresponding MD simulations as well as the scattering of MM-PBSA results for several simulations with slightly different starting conformations.

One should note that the different $\Delta G^{0\prime}$ values for bornyl caffeate and fukinolic acid, since different entropy contributions to ligand binding would have to be considered for these dissimilar ligands, cannot be reasonably compared. Nevertheless, in principle MM-PBSA should be able to yield accurate absolute binding free energies suitable for comparing all kinds of different ligands.[19]

Conclusion

We have shown that a combination of ligand docking, continuum solvent free energy, and explicit solvent TI calculations can be used to propose a reasonable binding mode for bornyl caffeate to HNE. Important hydrogen bonds that anchor the ligand into the binding site were found and the placement of the hydrophobic ligand part into the protein S1 specificity pocket explains the need for ligand hydrophobicity. Accurate relative binding free energies for bornyl caffeate derivatives could be calculated, paving the way for subsequent virtual structural ligand modifications in search of stronger binding ligands and a better understanding of ligand binding to HNE. Our approach may be useful as a second step after virtual screening, when likely binding compounds have been identified, to obtain more detailed and reliable information about their binding modes and affinities than a simple fast docking can provide.

Methods

The ligand docking calculations were performed with FlexX 1.13, a program designed for the docking of small- to medium-sized organic molecules into protein binding sites.[21] During the docking procedure the protein structure is considered as rigid, whereas the ligand conformation is treated as flexible by allowing rotations around acyclic single bonds. Bond lengths and angles are kept constant as given in the input structure. The docking algorithm incorporated in FlexX is based on matching complementary functional groups such as hydrogen bond donors and acceptors. It favors sterically restrictive interactions such as salt bridges and hydrogen bonds.[22] The ligand is placed into the binding site by an incremental construction algorithm. An empirically derived scoring function, based on the Böhm function,[23] is used to calculate the binding score, which gives an estimate of the binding free energy. The algorithm is described in detail in refs 21 and 24.

The ligand structures were sketched by hand and minimized using Hyperchem[25] prior to docking. For the protein structure the Protein Data Bank[26] crystal structure 1HNE was used after adding hydrogen atoms and optimizing them using the HB2NET module of the program WhatIf.[27]

All molecular dynamics simulations were carried out using the Amber8 molecular modeling suite.[28] Force field parameters used were ff03[29] for the protein parts of the system, gaff[30] for the ligands, and the TIP3P[31] model for water molecules. Ligand partial charges were derived by the RESP methodology[32] using Gaussian98[33] for quantum mechanical calculations on the HF/6-31G* level.

The protein ligand complexes were subjected to the following procedure prior to molecular dynamics data collection: The complexes were surrounded by a 12 Å layer of pre-equilibrated water molecules and neutralized by adding Cl^- ions. After 1000 steps of preliminary minimization, the system temperature was raised to 300 K by a Berendsen-type[34] coupling algorithm during 50 ps of constant volume dynamics with 10 kcal/mol·Å^2 restraints on all solute atoms. Finally, 150 ps of constant pressure dynamics were applied for volume equilibration. A time step of 2 fs in combination with the SHAKE[35] algorithm to constrain bond lengths involving hydrogen atoms was used for all simulations.

Molecular dynamics snapshots taken at 10 ps intervals and stripped of all counterions and water molecules were used as structural ensembles for evaluation by the MM-PBSA method as detailed in refs 36−38. In this approach, the binding energy of a ligand is calculated as

$$\Delta G^{0\prime}_{\mathrm{Bind}} = G^{0\prime}_{\mathrm{COM}} - (G^{0\prime}_{\mathrm{PROT}} + G^{0\prime}_{\mathrm{LIG}}) \quad (1)$$

where $G^{0\prime}_{\mathrm{COM}}$, $G^{0\prime}_{\mathrm{PROT}}$, and $G^{0\prime}_{\mathrm{LIG}}$ are the absolute free energies of the protein ligand complex, protein, and ligand respectively, each in aqueous solution, referring to the same arbitrary zero. Each of these contributions is calculated by averaging the total energy for each snapshot in the ensemble, calculated by

$$G^{0\prime} = E_{\mathrm{FF}} + \Delta G^0_{\mathrm{PB}} + \Delta G^0_{\mathrm{SA}} \quad (2)$$

E_{FF} represents the energy from the different force field terms for bond, angle, torsional, van der Waals, and electrostatic potential energies, and ΔG^0_{PB} is the polar contribution to the solvation free energy resulting from solving the Poisson−Boltzmann equation numerically. The pbsa Poisson−Boltzmann solver was used to determine this term. ΔG^0_{SA} represents the nonpolar contribution to the solvation free energy, estimated by a simple linear model based on the solvent accessible surface area (denoted as A_{SAS}) of the solute:

$$\Delta G^0_{\mathrm{SA}} = \alpha + A_{\mathrm{SAS}} \cdot \beta \quad (3)$$

The empirical parameters used to calculate ΔG^0_{SA}, α, and β were set to 0.092 kcal/mol and 0.00542 kcal/(mol*·Å^2), as in similar studies.[37]

The $G^{0\prime}_{\mathrm{Bind}}$ term in eq 1 does not include an estimate of the entropy contribution to ligand binding and is thus not identical to the actual binding free energy. The entropy contribution could in principle be estimated by performing normal-mode analysis on the different molecular species. Since entropies calculated by such an approach have a rather wide margin of error and entropy effects should be neglectable for a comparison of binding energies for different conformations of one ligand bound to the protein, no such correction of the $G^{0\prime}$ terms was performed.

The relative binding free energies for different ligands were computed by a more traditional computational approach, thermodynamic integration calculations.[39,40] By computing the free energy cost of transforming one ligand into another, both in the protein-bound and unbound (aqueous solution) states, one can calculate

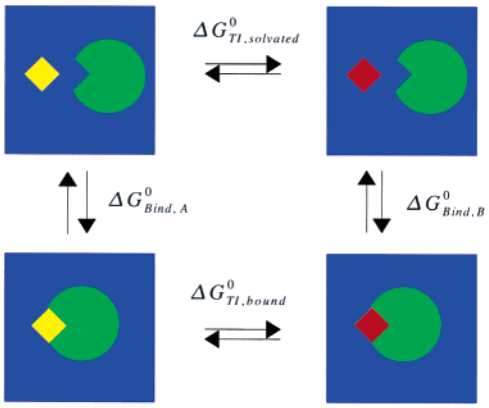

Figure 5. Thermodynamic cycle for calculation of the relative binding free energies for two different ligands A and B, depicted in yellow and red, respectively. The quantities $\Delta G^0_{\mathrm{Bind,A}}$ and $\Delta G^0_{\mathrm{Bind,B}}$ refer to the corresponding binding free energies of these ligands, whereas $\Delta G^0_{\mathrm{TI,bound}}$ and $\Delta G^0_{\mathrm{TI,solvated}}$ are the changes in free energy of transforming the ligands in the bound and solvated (unbound) state, respectively. The relative binding free energy can thus be computed according to eq 4.

the binding free energy difference of the two ligands using a simple thermodynamic cycle (Figure 5):

$$\Delta\Delta G^0_{\mathrm{Bind}} = \Delta G^0_{\mathrm{Bind,A}} - \Delta G^0_{\mathrm{Bind,B}} = \Delta G^0_{\mathrm{TI,solvated}} - \Delta G^0_{\mathrm{TI,bound}} \quad (4)$$

where $\Delta\Delta G^0_{\mathrm{Bind}}$ is the relative binding free energy of two ligands, $\Delta G^0_{\mathrm{Bind,A}}$ and $\Delta G^0_{\mathrm{Bind,B}}$ are the two binding free energies for the two ligands A and B, respectively, and ΔG^0_{TI} is the free energy difference for transforming the ligands into each other in the bound and solvated (unbound) states.

Each TI calculation was divided into two steps, the first of which corresponded to a transformation of the ligand partial charges to their perturbed state and the second one to the change of bond and atom types as well as vdW parameters. To avoid the "origin singularity" effect, in which the derivative of the potential energy becomes undefined when $\lambda = 1$ is reached, which is known to occur if vanishing or appearing atoms are simulated,[41] the following mixing rule for the perturbed and unperturbed potential functions was used:

$$V(\lambda) = (1-\lambda)^k V_0 + [1-(1-\lambda)^k]V_1 \quad (5)$$

where $V(\lambda)$ is the combined potential function used to describe the system properties at various values for λ, the perturbation variable. V_0 and V_1 are the potential functions for the unperturbed ($\lambda = 0$) and perturbed ($\lambda = 1$) state, respectively. Equation 5 with a value of $k = 4$ was used as the mixing rule for cases that did involve vanishing atoms, while a value of $k = 1$ was used in other cases. Setting $k = 1$ is equivalent to using linear mixing of the potential functions. All simulations were set up in a way that the transition of λ from 0 to 1 corresponds to the disappearance of atoms because using a potential function mixing rule as in eq 5 does not prevent the "origin singularity" effect from occurring in cases where atoms appear (on the contrary, the effect would be even more pronounced).

The $dV/d\lambda$ integral was solved numerically by computing the weighted average of five $dV/d\lambda$ values. A 100 ps simulation with preceding 50 ps of equilibration using the same parameters as detailed above was performed for each value of λ. The difference in free energy is given by

$$\Delta G^0 = G_1{}^0 - G_0{}^0 \approx \int_{\lambda=0}^{1} \left\langle \frac{\partial V}{\partial \lambda} \right\rangle_\lambda d\lambda \approx \sum_{i=1}^{5} w_i \left\langle \frac{\partial V}{\partial \lambda} \right\rangle_{\lambda_i} \quad (6)$$

where $G_1{}^0$ and $G_0{}^0$ refer to the free energies of the perturbed und unperturbed states, respectively. The weights w_i were chosen as described in the Amber manual.[28]

Abbreviations: rmsd, root-mean-square deviation; TI, thermodynamic integration; HNE, human neutrophile elastase; MD, molecular dynamics; MM-PBSA, molecular mechanics-Poisson Boltzmann surface area.

Acknowledgment. Funding for this work was provided by the German Academic Exchange Service (Grant #332400109) and the Landesgraduiertenförderung Baden-Württemberg (AZ: ZSA1.3-7631.0). D.A.C. was supported by NIH grant GM56531. The authors wish to thank the Amber user community for helpful and interesting discussions. A.L. and T.S. wish to thank Prof. P. Gräber for his ongoing support and Prof. I. Merfort for her continuing interest in our work and helpful discussions.

Supporting Information Available: Examples of a solvated and neutralized protein ligand complex structure, as pdb files, for one of the bornyl caffeate placement group 2 complexes after ligand docking, after the 200 ps equilibration, and at the end of a 1 ns MD simulation. This material is available free of charge via the Internet at http://pubs.acs.org.

References

(1) Belaaouaj, A. Neutrophil elastase-mediated killing of bacteria: lessons from targeted mutagenesis. *Microbes Infect.* **2002**, *12*, 1259−1264.
(2) Weinrauch, Y.; Drujan, D.; Shapiro, S. D.; Weiss, J.; Zychlinsky, A. Neutrophil elastase targets virulence factors of enterobacteria. *Nature* **2002**, *417*, 91−94.
(3) Bode, W.; Wei, A.-Z.; Huber, R.; Meyer, E.; Travis, J.; Neumann, S. X-ray crystal structure of the complex of human leukocyte elastase (PMN elastase) and the third domain of the turkey ovomucoid inhibitor. *EMBO J.* **1986**, *5*, 2453−2458.
(4) Sinha, S.; Watorek, W.; Karr, S.; Giles, J.; Bode, W.; Travis, J. Primary structure of human neutrophil elastase. *Proc. Natl. Acad. Sci. U.S.A.* **1987**, *84*, 2228−2232.
(5) Navia, M. A.; McKeever, B. M.; Springer, J. P.; Lin, T.-Y.; Williams, H. R.; Fluder, E. M.; Dorn, C. P.; Hoogsteen, K. Structure of human neutrophil elastase in complex with a peptide chloromethyl ketone inhibitor at 1.84-Å resolution. *Proc. Natl. Acad. Sci. U.S.A.* **1989**, *86*, 7−11.
(6) Cregge, R. J.; Durham, S. L.; Farr, R. A.; Gallion, S. L.; Hare, C. M.; Hoffman, R. V.; Janusz, M. J.; Kim, H. O.; Koehl, J. R.; Mehdi, S.; Metz, W. A.; Peet, N. P.; Pelton, J. T.; Schreuder, H. A.; Sunder, S.; Tardif, C. Inhibition of human neutrophil elastase. 4. Design, synthesis, X-ray crystallographic analysis, and structure−activity relationships for a series of P2-modified, orally active peptidyl pentafluoroethyl ketones. *J. Med. Chem.* **1998**, *41*, 2461−2480.
(7) Macdonald, S. J. F.; Dowle, M. D.; Harrison, L. A.; Clarke, G. D. E.; Inglis, G. G. A.; Johnson, M. R.; Shah, P.; Smith, R. A.; Amour, A.; Fleetwood, G.; Humphreys, D. C.; Molloy, C. R.; Dixon, M.; Godward, R. E.; Wonacott, A. J.; Singh, O. M. P.; Hodgson, S. T.; Hardy, G. W. Discovery of further pyrrolidine *trans*-lactams as inhibitors of human neutrophil elastase (HNE) with potential as development candidates and the crystal structure of HNE complexed with an inhibitor (GW475151). *J. Med. Chem.* **2002**, *45*, 3878−3890.
(8) Ohbayashi, H. Neutrophil elastase inhibitors as treatment for COPD. *Expert Opin. Investig. Drugs* **2002**, *11*, 965−980.
(9) Bernstein, P. R.; Edwards, P. D.; Williams, J. C. Inhibitors of human leukocyte elastase. *Prog. Med. Chem.* **1994**, *31*, 59−120.
(10) Döring, G. The role of neutrophil elastase in chronic inflammation. *Am. J. Respir. Crit. Care Med.* **1994**, *150*, S114−S117.
(11) Melzig, M. F.; Löser, B.; Lobitz, G. O.; Tamayo-Castillo, G.; Merfort, I. Inhibition of granulocyte elastase activity by caffeic acid derivatives. *Pharmazie* **1999**, *54*, 712−712.
(12) Löser, B.; Kruse, S. O.; Melzig, M. F.; Nahrstedt, A. Inhibition of neutrophil elastase activity by cinnamic acid derivatives from *Cimicifuga racemosa*. *Planta Med.* **2000**, *66*, 751−753.
(13) Siedle, B.; Murillo, R.; Hucke, O.; Labahn, A.; Merfort, I. Structure activity relationship studies of cinnamic acid derivatives as inhibitors of human neutrophil elastase revealed by ligand docking calculations. *Pharmazie* **2003**, *58*, 337−339.
(14) Kollman, P. Free energy calculations: Applications to chemical and biochemical phenomena. *Chem. Rev.* **1993**, *93*, 2395−2417.
(15) Lamb, M. L.; Jorgensen, W. L. Computational approaches to molecular recognition. *Curr. Opin. Chem. Biol.* **1997**, *1*, 449−457.
(16) Simonson, T.; Archontis, G.; Karplus, M. Continuum treatment of long-range interactions in free energy calculations. Application to protein−ligand binding. *J. Phys. Chem. B* **1997**, *101*, 8349−8362.

(17) Torrie, G. M.; Valleau, J. P. Nonphysical sampling distributions in Monte Carlo free-energy estimation: umbrella sampling. *J. Comput. Phys.* **1977**, *23*, 187−199.
(18) Lin, J.-H.; Perryman, A. L.; Schames, J. R.; McCammon, J. A. The relaxed complex method: Accommodating receptor flexibility for drug design with an improved scoring scheme. *Biopolymers* **2003**, *68*, 47−62.
(19) Kuhn, B.; Kollman, P. A. Binding of a diverse set of ligands to avidin and streptavidin: An accurate quantitative prediction of their relative affinities by a combination of molecular mechanics and continuum solvent models. *J. Med. Chem.* **2000**, *43*, 3786−3791.
(20) Verma, R. P.; Hansch, C. An approach towards the quantitative structure−activity relationships of caffeic acid and its derivatives. *ChemBioChem.* **2004**, *5*, 1188−1195.
(21) Rarey, M.; Kramer, B.; Lengauer, T.; Klebe, G. A fast flexible docking method using an incremental construction algorithm. *J. Mol. Biol.* **1996**, *261*, 470−489.
(22) Rarey, M.; Kramer, B.; Lengauer, T. Docking of hydrophobic ligands with interaction-based matching algorithms. *Bioinformatics* **1999**, *15*, 243−250.
(23) Böhm, H.-J. The development of a simple empirical scoring function to estimate the binding constant for a protein−ligand complex of known three-dimensional structure. *J. Comput. Aided Mol. Des.* **1994**, *8*, 243−256.
(24) Kramer, B.; Rarey, M.; Lengauer, T. Evaluation of the FLEXX incremental construction algorithm for protein−ligand docking. *Proteins* **1999**, *37*, 228−241.
(25) *Hyperchem Release 6*, Hypercube Inc., 2000.
(26) Berman, H. M.; Westbrook, J.; Feng, Z.; Gilliland, G.; Bhat, T. N.; Weissig, H.; Shindyalov, I. N.; Bourne, P. E. The Protein Data Bank. *Nucleic Acids Res.* **2000**, *28*, 235−242.
(27) Vriend, G. WHAT IF: a molecular modeling and drug design program. *J. Mol. Graph.* **1990**, *8*, 52−56.
(28) Case, D. A.; Darden, T. A.; Cheatham, T. E., III; Simmerling, C. L.; Wang, J.; Duke, R. E.; Luo, R.; Merz, K. M.; Wang, B.; Pearlman, D. A.; Crowley, M.; Brozell, S.; Tsui, V.; Gohlke, H.; Mongan, J.; Hornak, V.; Cui, G.; Beroza, P.; Schafmeister, C.; Caldwell, J. W.; Ross, W. S.; Kollman, P. A. *AMBER 8*, University of California, San Francisco, 2004.
(29) Duan, Y.; Wu, C.; Chowdhury, S.; Lee, M. C.; Xiong, G.; Zhang, W.; Yang, R.; Cieplak, P.; Luo, R.; Lee, T.; Caldwell, J.; Wang, J.; Kollman, P. A point-charge force field for molecular mechanics simulations of proteins based on condensed-phase quantum mechanical calculations. *J. Comput. Chem.* **2003**, *24*, 1999−2012.
(30) Wang, J.; Wolf, R. M.; Caldwell, J. W.; Kollman, P. A.; Case, D. A. Development and testing of a general Amber force field. *J. Comput. Chem.* **2004**, *25*, 1157−1174.
(31) Jorgensen, W. L.; Chandrasekhar, J.; Madura, J. D.; Impey, R. W.; Klein, M. L. Comparison of simple potential functions for simulating liquid water. *J. Chem. Phys.* **1983**, *79*, 926−935.
(32) Bayly, C. I.; Cieplak, P.; Cornell, W. D.; Kollman, P. A. A well-behaved electrostatic potential based method using charge restraints for deriving atomic charges: the RESP model. *J. Phys. Chem.* **1993**, *97*, 10269−10280.
(33) Frisch, M. J. et al. *Gaussian98*, Gaussian Inc., 1998.
(34) Berendsen, H. J. C.; Postma, J. P. M.; van Gunsteren, W. F.; DiNola, A.; Haak, J. R. Molecular dynamics with coupling to an external bath. *J. Chem. Phys.* **1984**, *81*, 3684−3690.
(35) Ryckaert, J.-P.; Ciccotti, G.; Berendsen, H. J. C. Numerical integration of the cartesian equations of motion of a system with constraints: molecular dynamics of *n*-alkanes. *J. Comput. Phys.* **1977**, *23*, 327−341.
(36) Kollman, P. A.; Massova, I.; Reyes, C.; Kuhn, B.; Huo, S.; Chong, L.; Lee, M.; Lee, T.; Duan, Y.; Wang, W.; Donini, O.; Cieplak, P.; Srinivasan, J.; Case, D. A.; Cheatham, T. E., III Calculating structures and free energies of complex molecules: combining molecular mechanics and continuum models. *Acc. Chem. Res.* **2000**, *33*, 889−897.
(37) Srinivasan, J.; Cheatham, T. E., III; Cieplak, P.; Kollman, P. A.; Case, D. A. Continuum solvent studies of the stability of DNA, RNA, and phosphoramidate-DNA helices. *J. Am. Chem. Soc.* **1998**, *120*, 9401−9409.
(38) Ni, H.; Sotriffer, C. A.; McCammon, J. A. Ordered water and ligand mobility in the HIV-1 integrase-5CITEP complex: a molecular dynamics study. *J. Med. Chem.* **2001**, *44*, 3043−3047.
(39) Gouda, H.; Kuntz, I. D.; Case, D. A.; Kollman, P. A. Free energy calculations for theophylline binding to an RNA aptamer: Comparison of MM-PBSA and thermodynamic integration methods. *Biopolymers* **2003**, *68*, 16−34.
(40) Miyamoto, S.; Kollman, P. A. Absolute and relative binding free energy calculations of the interaction of biotin and its analogs with streptavidin using molecular dynamics/free energy perturbation approaches. *Proteins* **1993**, *16*, 226−245.
(41) Simonson, T. Free energy of particle insertion: An exact analysis of the origin singularity for simple liquids. *Mol. Phys.* **1993**, *80*, 441−447.

JM0505720